

ER cross section measurement in $^{16}\text{O}+^{194}\text{Pt}$ reaction using gas-filled mode of HYRA

E. Prasad^{1,2,a}, K.M. Varier¹, N. Madhavan³, S. Nath³, J. Gehlot³, Sunil Kalkal⁴, Jhilaam Sadhukhan⁵, G. Mohanto³, P. Sugathan³, A. Jhingan³, B.R.S. Babu¹, T. Varughese³, K.S. Golda³, B.P. Ajith Kumar³, B. Satheesh¹, Santanu Pal⁵, R. Singh⁴, A. K. Sinha⁶, and S. Kailas⁷

¹ Department of Physics, University of Calicut, Calicut 673635, India

² Department of Physics, Govt. College Kasaragod, Vidhyanagar, 671123, India

³ Inter University Accelerator Centre, Aruna Asaf Ali Marg, New Delhi 110067, India

⁴ Department of Physics and Astrophysics, Delhi University, Delhi 110007, India

⁵ Physics Group, Variable Energy Cyclotron Centre, 1/AF Bidhan Nagar, Kolkata 700064, India

⁶ UGC-DAE CSR, Kolkata Centre, 3/LB-8, Bidhan Nagar, Kolkata 700098, India

⁷ Nuclear Physics Division, Bhabha Atomic Research Centre, Mumbai 400085, India

Abstract. Evaporation residue (ER) excitation function in the complete fusion of ^{16}O with ^{194}Pt is measured around the Coulomb barrier using gas-filled mode of the HYbrid Recoil mass Analyser (HYRA) at the Inter University Accelerator Centre (IUAC), New Delhi. Measured ER excitation function is compared with statistical model calculation. Nuclear dissipation strength $\beta = 1.5$ is required to explain the experimental data at higher excitation energies.

1 Introduction

Heavy ion fusion reactions provide important information on the dynamics and decay of hot nuclear matter. At moderate excitation energies, the compound nucleus (CN) decay mainly via particle evaporation and fission. ERs are the true signatures of the CN formation and can be used as an excellent probe for exploring the onset of non-compound nuclear processes as well as nuclear dissipation. Onset of dissipative forces causes hindrance to fission, which is reflected in enhancement of ER cross section over the predictions of standard statistical model. On the other hand, non-compound nuclear processes hinder the formation of the CN. This is manifested in reduction of ER cross section. In this way, ER excitation function can be used as a powerful tool to understand the fusion-fission mechanism in heavy systems. We here report the ER excitation function measurement in the complete fusion of ^{16}O with ^{194}Pt at beam energies near and above the Coulomb barrier.

2 The Experiment

The experiment was performed at the 15 UD Pelletron accelerator facility of the IUAC, New Delhi. Pulsed ^{16}O beam with a pulse separation of $4\ \mu\text{s}$ was used in the experiment to bombard an isotopically enriched ^{194}Pt (96.5% enrichment) target of thickness $300\ \mu\text{g}/\text{cm}^2$ on a $20\ \mu\text{g}/\text{cm}^2$ thick carbon backing. ER excitation function measurements were

carried out at laboratory beam energies of 75.4, 79.5, 83.7, 87.8, 91.9, 96.0, 101.1 and 103.1 MeV. ERs produced in the reaction were separated from the intense beam background using the first stage of the recoil separator HYRA [1], operated in gas-filled mode, and transported to its focal plane. HYRA is a dual mode, dual stage recoil mass separator/spectrometer with its first stage operable with momentum dispersion in the gas-filled mode and as a momentum achromat in the vacuum mode. The electromagnetic configuration of the same is $Q_1Q_2\text{-MD}_1\text{-}Q_3\text{-MD}_2\text{-}Q_4Q_5$, where Q stands for magnetic quadrupole and MD stands for magnetic dipole, respectively. Fig. 1 shows the schematic representation of the first stage of the HYRA. Gas-filled separators provide better transmission efficiency for ions in comparison to vacuum mode spectrometers due to their inherent velocity and charge state focusing caused by multiple collisions with the gas molecules. This aspect is particularly useful for reactions where ER cross section is a small fraction of total fusion cross section. Under optimized gas pressure and magnetic field values, the particles follow a mean trajectory decided by the mean charge state. We used a simulation code, developed in-house [2], to calculate the mean charge state and magnetic field values. The HYRA was filled with helium gas and an optimum pressure of 0.15 Torr was maintained throughout the experiment. This value was obtained by maximizing the normalized ER yield at the focal plane in the beginning of the experiment.

The reaction $^{16}\text{O}+^{194}\text{Pt}$ being very asymmetric, ERs are formed with very low recoil energies. These low energy ERs reaching the focal plane were detected using a po-

^a e-mail: prasad.e.nair@gmail.com

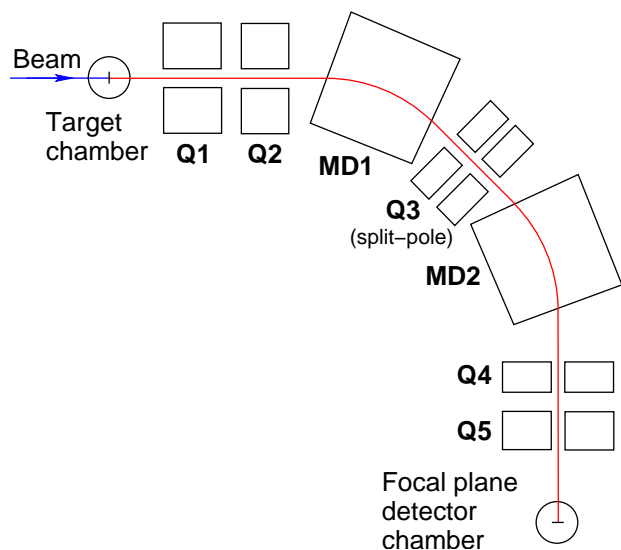


Fig. 1. The schematic representation of the first stage of the HYRA used in the present study. Q and MD stand for magnetic quadrupole and magnetic dipole, respectively.

sition sensitive multi-wire proportional counter (MWPC) with an active area of $57 \times 57 \text{ mm}^2$ followed by a two-dimensional position sensitive silicon detector (SSBD) with an active area of $50 \times 50 \text{ mm}^2$. The MWPC was operated with isobutane gas at a pressure ~ 2 mbar. It provided position signals (both X and Y), energy loss signal (from the cathode) and timing signal (from the anode). The position signals were taken from the two ends of the X and Y plane wire-frames through delay-line chips. These were processed through constant fraction discriminators (CFDs) and fed to the time to digital converter (TDC) as stop signals. Anode timing signal was used as the common start of the TDC. Two silicon detectors, mounted inside the target chamber at $\pm 22^\circ$ with respect to the beam direction, were used to record the elastically scattered beam particles for absolute normalization of ER cross section. These detectors along with beam current maximization in the beam catcher helped in reproducibly positioning beam at the center of the target.

For effectively separating slowly moving ERs, from the target-like and the beam-like particles, a time of flight (TOF) spectrum was generated with anode signal as the start and radio frequency (RF) signal (used for beam pulsing) as the stop. It was observed that the probable contamination at the focal plane, originating from the scattered events, was less than 1.5%, at 101.1 MeV beam energy. We could not use pulsed beam due to low beam current at 103.1 MeV and hence could not quantify the contamination at the focal plane. However, the same was expected to be less than 1.5% because of the lower scattering cross section [3] at this energy. Two-dimensional plot of energy versus TOF for the reaction $^{16}\text{O} + ^{194}\text{Pt}$ at 101.1 MeV beam energy is shown in Fig. 2. ERs are seen at the center and

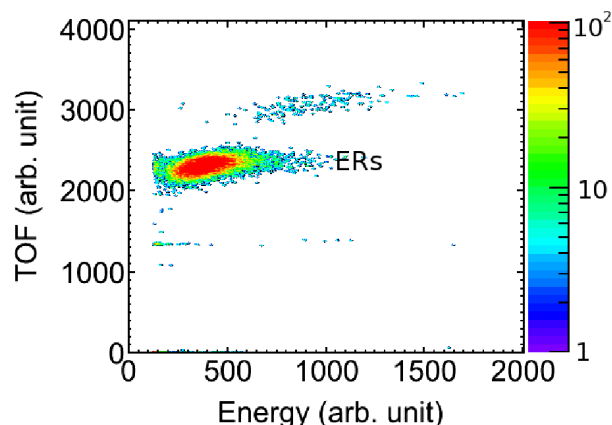


Fig. 2. Two-dimensional plot of energy versus TOF for $^{16}\text{O} + ^{194}\text{Pt}$ at 101.1 MeV beam energy.

the scattered events are very well separated from the ERs. The IUAC data sorting software CANDLE [4] was used for collecting and analyzing the data.

3 Data Analysis and Results

The total ER cross section is given by

$$\sigma_{\text{ER}} = \frac{Y_{\text{ER}}}{Y_{\text{M}}} \left(\frac{d\sigma}{d\Omega} \right)_{\text{R}} \Omega_{\text{M}} \frac{1}{\epsilon_{\text{HYRA}}} \quad (1)$$

where Y_{ER} is the ER yield at the focal plane, Y_{M} is the yield at the monitor detector, ϵ_{HYRA} is the HYRA transmission efficiency and Ω_{M} is the solid angle subtended by the monitor detector. $\left(\frac{d\sigma}{d\Omega} \right)_{\text{R}}$ is the differential Rutherford scattering cross section in the laboratory system.

Transmission efficiency is a major concern in ER measurements using recoil mass separators/spectrometers. It is the ratio of the number of ERs detected by the focal plane detector to the total number of ERs produced at the target chamber. It depends on various factors [5] such as entrance channel mass asymmetry, beam energy, target thickness, exit channel of interest, angular acceptance of the HYRA, magnetic field and gas pressure settings of the HYRA and size of the focal plane detector. Conventional γ -ray method to determine transmission efficiency was not very effective in the present measurement due to the intense γ -ray background originating from fission fragments as well as the nickel window foil, used for separating the gas medium from the high vacuum of the beam line. Hence we used $^{16}\text{O} + ^{184}\text{W}$ as the calibration reaction, for which ER cross sections were already reported [6], for determining transmission efficiency of the HYRA for $^{16}\text{O} + ^{194}\text{Pt}$ reaction.

Isotopically enriched ^{184}W target [7] was bombarded by ^{16}O beam at 96.0 MeV beam energy. $\epsilon_{\text{HYRA}}^{\text{MWPC}}$ for this reaction was then calculated, using the ER cross section from Ref. [6], which was found to be $2.48 \pm 0.40\%$ when the ER yields were taken from the MWPC detector. $\epsilon_{\text{HYRA}}^{\text{SSBD}}$ obtained with the ER counts from the silicon detector for the

same reaction was $1.78 \pm 0.27\%$. In a gas-filled recoil separator, the separated reaction products (here, ERs) are not tightly focused on the focal plane detector. Because of this, a large area detector is preferred. The area of the SSBD used in our experiment was not sufficient to record all the ERs reaching the focal plane. The MWPC, on the other hand, had larger area and could record more ERs compared to the SSBD. The difference in efficiency is simply the manifestation of the difference in the active area of the two detectors. The transmission efficiency for $^{16}\text{O}+^{194}\text{Pt}$ reaction is then extracted by comparing the normalized angular distributions of the ERs from the two reactions, simulated using the semi-microscopic Monte Carlo code TERS [8] and shown in Fig. 3. The simulation was performed for the major ER channels (4n, 5n and 6n evaporation) in the case of $^{16}\text{O}+^{184}\text{W}$ reaction at 96.0 MeV beam energy. The total angular distribution was normalized using relative population (10%, 80% and 7% for 4n, 5n and 6n evaporation, respectively) of the exit channels. Similar method was followed for $^{16}\text{O}+^{194}\text{Pt}$ reaction at different beam energies. The relative population of ERs for both the reactions were obtained using the statistical model code PACE3 [9]. It may be noticed that the angular distributions of ERs from $^{16}\text{O}+^{194}\text{Pt}$ at different beam energies are quite similar. But there is significant difference in angular distributions be-

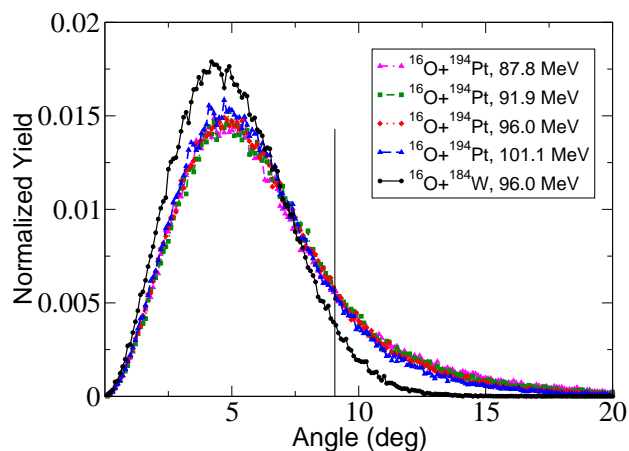


Fig. 3. The normalized angular distributions of ERs from $^{16}\text{O}+^{194}\text{Pt}$ and $^{16}\text{O}+^{184}\text{W}$ reactions simulated using the Monte Carlo code TERS. The line at 9.6° indicates the angular opening of the first quadrupole magnet in HYRA.

At 96.0 MeV beam energy, the area under the total angular distribution curve for $^{16}\text{O}+^{194}\text{Pt}$ reaction was approximately 10% less than that for $^{16}\text{O}+^{184}\text{W}$ reaction, within the angular acceptance of the HYRA (polar angle 9.6°). This reduction in area was expected for $^{16}\text{O}+^{194}\text{Pt}$ reaction, due to its more asymmetric entrance channel compared to the latter reaction. Hence, at 96.0 MeV beam energy, $\epsilon_{\text{HYRA}}^{\text{SSBD}}$ for $^{16}\text{O}+^{194}\text{Pt}$ was found to be $1.60 \pm 0.24\%$. In a similar way, $\epsilon_{\text{HYRA}}^{\text{SSBD}}$ at other beam energies were obtained by comparing the normalized angular distributions. Variation in ϵ_{HYRA} with beam energy was not very significant, in

the beam energy range of the present study. Hence, cross section estimation was done with $\epsilon_{\text{HYRA}} = 1.60 \pm 0.24\%$. The overall errors in the estimated cross sections are $\leq 20\%$, out of which ϵ_{HYRA} contributes the maximum.

We must point out here that the method of estimating ϵ_{HYRA} , followed in this work, relies on an assumption. We assume that the HYRA acceptance in energy and charge state is nearly 100% and the only major factor that causes difference in transmission efficiency for different reactions is the angular distribution (and hence angular acceptance) of the ERs. This assumption is quite justified as we carefully optimized the magnetic field values and gas pressure to achieve charge state and velocity focusing.

4 Statistical Model Calculation

Having the experimental ER cross sections in hand, statistical model calculation has been performed, assuming that the system forms a CN after capture of the projectile nucleus into the target nucleus and the contribution from the non-compound nuclear processes such as quasifission and fastfission are negligible. The CN decays via particle evaporation (mainly neutron, proton and α -particle), giant dipole resonance (GDR) γ -emission and fission. All these decay modes are considered in the present statistical model code.

Initially we have performed the model calculation using the fission width (Γ_{BW}) taken from the transition state model of Bohr and Wheeler [10], which is given as

$$\Gamma_{\text{BW}} = \frac{1}{2\pi\rho_g(E_i)} \int_0^{E_i - V_B} \rho_s(E_i - V_B - \epsilon) d\epsilon \quad (2)$$

where ρ_g and ρ_s are the level densities at the initial state (E_i, l_i) and the saddle point, respectively. E_i is the excitation energy and l_i is the spin of the CN, where the subscript i stands for the initial state. V_B is the fission barrier height calculated from the finite-range liquid drop model for nuclear potential [11]. The energy dependent form of the level density parameter a [12] was used in the present calculation.

The model calculation [13] has been performed using the fusion spin distribution as the input. The fusion cross section is taken as the sum of ER cross section and fission cross section at each beam energy. The fusion spin distribution is then obtained from the coupled-channels code CCFULL [14] by reproducing the experimental total fusion cross section. The experimental fission cross-sections for $^{16}\text{O}+^{194}\text{Pt}$ reaction upto $E_{\text{lab}} = 90$ MeV are measured in a separate experiment [15]. At higher beam energies CCFULL predictions for total fusion cross section are used. The model calculation with Γ_{BW} underpredicted ER cross sections, especially at higher excitation energies.

In order to incorporate the effect of nuclear dissipation, statistical model calculation is undertaken using the Kramers' formula for the fission width Γ_K , which is given by [16]

$$\Gamma_K = \frac{\hbar\omega_g}{2\pi} e^{-V_B/T} (\sqrt{1 + \beta^2} - \beta). \quad (3)$$

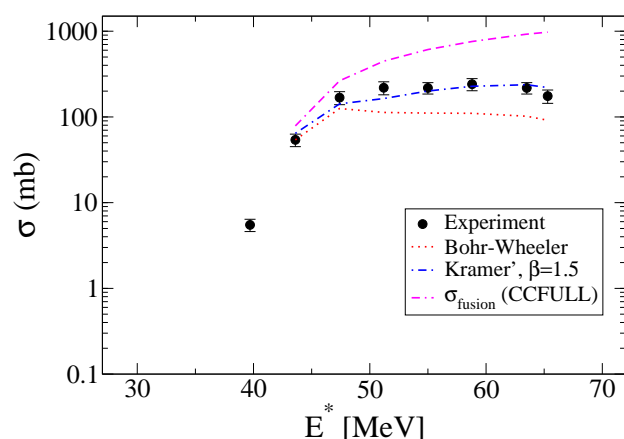


Fig. 4. The experimental ER cross sections for $^{16}\text{O}+^{194}\text{Pt}$ reaction compared with statistical model calculation assuming Bohr-Wheeler as well as Kramers' fission widths. Total fusion cross sections calculated using CCFULL is also shown.

Here β denotes the dissipation strength and ω_g is the measure of the potential curvature at the ground state configuration. The temperature T is evaluated using the Fermi gas model. As we do not have fission cross sections at below barrier energies, the calculation is restricted to above barrier energies only. Statistical model calculation with a dissipation strength of $\beta = 1.5$ can reasonably explain ER cross sections. In Fig. 4 we compare the experimental data with model calculation assuming Bohr-Wheeler and Kramers' fission widths.

5 Discussion

The present study shows that a dissipative strength of $\beta = 1.5$ is required to fit the experimental ER data in the complete fusion of ^{16}O with ^{194}Pt . This result provides further evidence of onset of nuclear dissipation in mass ~ 200 region. Shidling et al [6] reported that a dissipative strength of $\beta = 3$ is required to explain ER excitation function in $^{16}\text{O}+^{184}\text{W}$ reaction. Similar results were reported in Ref. [17]. In all these works including the present measurement, a constant β -value reasonably fits the experimental data in 50-80 MeV excitation energy. However, excitation energy dependent β -values were reported for $^{32}\text{S}+^{182}\text{W}$ reaction at 85 -135 MeV excitation energy [18]. It is hence very important to understand the excitation energy dependence of the dissipation strength in mass ~ 200 region. This calls for more study over a wide range of excitation energies in this mass region.

References

1. N. Madhavan, S. Nath, T. Varughese, J. Gehlot, A. Jhingan, P. Sugathan, A.K. Sinha, R. Singh, K.M. Varier, M.C. Radhakrishna, E. Prasad, S. Kalkal, G.

- Mohanto, J.J. Das, Rakesh Kumar, R.P. Singh, S. Muralithar, R.K. Bhowmik, A. Roy, Rajesh Kumar, S.K. Suman, A. Mandal, T.S. Datta, J. Chako, A. Choudhury, U.G.Naik, A.J. Malyadri, M. Archunan, J. Zacharias, S. Rao, Mukesh Kumar, P. Barua, E.T. Subramanian, K. Rani, B.P. Ajith Kumar and K.S. Golda, *Pramana* **75**, 317 (2010).
2. S. Nath and N. Madhavan, *IUAC Annual Report*, Section 4.3.3, p. 103, (2006-2007).
3. W.U. Schroder and J.R. Huizenga, in *Damped Nuclear Reactions, Treatise on Heavy-ion Science*, edited by D. A. Bromley (Plenum Press, New York, 1984), Vol.2, p.115.
4. E.T. Subramaniam, B.P. Ajith Kumar and R.K. Bhowmik, Collection and Analysis of Nuclear Data using Linux nEtnet (unpublished).
5. S. Nath, P.V. Madhusudhana Rao, Santanu Pal, J. Gehlot, E. Prasad, Gayatri Mohanto, Sunil Kalkal, Jhilmam Sadhukhan, P.D. Shidling, K.S. Golda, A. Jhingan, N. Madhavan, S. Muralithar and A. K. Sinha, *Phys. Rev C* **81**, 064601 (2010).
6. P.D. Shidling, N.M. Badiger, S. Nath, R. Kumar, A. Jhingan, R.P. Singh, P. Sugathan, S. Muralithar, N. Madhavan, A.K. Sinha, Santanu Pal, S. Kailas, S. Verma, K. Kalita, S. Mandal, R. Singh, B.R. Behera, K.M. Varier and M.C. Radhakrishna, *Phys. Rev C* **74**, 064603 (2006).
7. P.D. Shidling, S.R. Abhilash, D. Kabiraj, and N. Madhavan, *Nucl. Instr. and Meth. A* **590**, 79 (2008).
8. S. Nath, *Comput. Phys. Commun.* **180**, 2392 (2009).
9. A. Gavron, *Phys. Rev. C* **21**, 230 (1980).
10. N. Bohr and J.A. Wheeler, *Phys. Rev.* **56**, 426 (1936).
11. A. J. Sierk, *Phys. Rev. C* **33**, 2039 (1986).
12. A.V. Ignatyuk, M.G. Itkis, V.N. Okolovich, G.N. Smirenki and A. Tishin, *Sov. J. Nucl. Phys.* **21**, 255 (1975).
13. Jhilmam Sadhukhan and Santanu Pal, *Phys. Rev. C* **79**, 064606 (2009).
14. K. Hagino, N. Rowley and A.T. Kruppa, *Comput. Phys. Commun.* **123**, 143 (1999).
15. E. Prasad, K.M. Varier, R.G. Thomas, K. Mahata, A.M. Vinodkumar, S. Appannababu, P. Sugathan, K.S. Golda, B.R.S. Babu, A. Saxena, B.V. John and S. Kailas, *Proceedings of the DAE Symp. on Nucl. Phys* Vol.55, p310 (2010).
16. H.A. Kramers, *Physica (Amsterdam)* **7**, 284 (1940).
17. I. Dioszegi *Phys. Rev. C* **64**, 019801 (2001).
18. B.B. Back, D.J. Blumenthal, C.N. Davids, D.J. Henderson, R. Hermann, D.J. Hofman, C.L. Jiang, H.T. Penttila, and A.H. Wuosmaa, *Phys. Rev. C* **60**, 044602 (1999).